ASTRONOMY & ASTROPHYSICS
SUPPLEMENT SERIES

Astron. Astrophys. Suppl. Ser. **114,** 565-574 (1995)

New measurements of radial velocities in clusters of galaxies. IV.*

D. Proust[1], A. Mazure[2], C. Vanderriest[3], L. Sodré Jr.[4] and H.V. Capelato[5]

[1] Observatoire de Paris, Section de Meudon, DAEC, F-92195 Meudon Cedex, France
[2] Laboratoire d'Astronomie Spatiale, Les Trois Lucs, F-13012 Marseille, France
[3] Canada-France-Hawaii Telescope Corporation, P.O. Box 1597, Kamuela, HI 96743, U.S.A.
[4] Departamento de Astronomia IAG/USP, Caixa Postal 9638, 01065-970 Sao Paulo, Brazil
[5] Divisao de Astrofisica INPE/MCT, CP151, 12201 Sao José dos Campos, Brazil

Received June 9; accepted June 26, 1995

Abstract. — We have obtained 65 new redshifts in 4 Abell galaxy clusters as well as 15 velocities of galaxies observed through the galactic plane, at ESO and OHP. Data on individual galaxies are presented**, and the accuracy of the determined velocities are discussed as well as some properties of the clusters.

Key words: galaxies: redshift — galaxies: cluster of

1. Introduction

Redshift surveys in clusters of galaxies are needed to study their dynamical and evolutionary states, estimating parameters such as the mass, shape and distortion of the velocity field, presence of substructures or projected galaxies and groups, strength of dynamical friction and two-body processes and, in general, the present stage of their dynamical evolution. This information is useful not only to test scenarii of galaxy formation, but also of the formation and evolution of large structures. In clusters, the mean velocity is a key factor in deriving distances, permitting the study of matter distribution over very large scales. Within clusters the analysis of the velocity field can lead to an estimate of the virial mass, constraining models of the dark matter content. Galaxy velocity measurements provide information complementary to that obtained through X-ray observations of clusters. Both form basic pieces of information for the understanding of clusters. Here we examine the velocity and galaxy distribution in the clusters A 957, A 979, A 2040 and A 2063; additional observations concerning a few galaxies observed through the galactic plane are also presented. Section 2 presents the instrumentation and the the data reduction techniques and comparisons with previous measurements. In Sect. 3 analyses of A 957, A 979, A 2040, and A 2063 are performed.

*based on observations made at ESO, La Silla (Chile) and Haute-Provence Observatory, CNRS (France)
**Tables 1 and 2 are also available in electronic form at the CDS via anonymous ftp 130.79.128.5.

2. Observations and data reductions

The program of radial velocity measurements was carried out years ago, and some results have been already published (see e.g. Proust et al. 1987, 1988, 1992; Capelato et al. 1991). The new velocities has been obtained at the 1.50 m ESO telescope, La Silla (Chile), and at the 1.93 m telescope, Haute-Provence Observatory (France).

Observations with the 1.50 m ESO telescope were carried out in January 1992. We used the Boller and Chivens spectrograph at the Cassegrain focus, equipped with a 600 lines/mm grating blazed at 5000 Å and coupled to an RCA CCD (1024 × 640 pixels) detector with pixel size of 15 μm. A dispersion of 172 Å/mm was used, providing spectral coverage from 3750 to 5700 Å. The exposure times ranged between 30 and 60 min. according to the magnitude of the object. During the run, calibration exposures were made before and after each galaxy observation using an He-Ar source. Observations with the 1.93 m telescope were carried out in April 1994; we used the CARELEC spectrograph at the Cassegrain focus, equipped with a 150 lines/mm grating blazed at 5000 Å and coupled to a Tektronix CCD (512^2 pixels) detector. A dispersion of 260 Å/mm was used, providing spectral coverage from 3600 to 7300 Å; obervations were made in the same conditions as the ESO ones.

We also observed in May 1991 with poor weather conditions with the multiobject spectrograph SILFID (Vanderriest & Lemonnier 1988) attached at the Cassegrain focus, equipped with drilled plates. Thirty separate optical fibers were available for collecting the light from galaxies spread over a field of 20 arcmin diameter

in the telescope focal plane; the technical specifications are given in Capelato et al. (1991). Additional observations carried out in July 1991 are also listed; they concern few galaxies observed through the galactic plane (see e.g. Kraan-Korteweg et al. 1994).

In the ESO run the stars HD 35410 (K0III) and CPD−43°2527 (K1III) (Maurice et al. 1984) were observed every night for the purpose of controlling the zero point in the velocity scale and for use as cross-correlation templates; the same procedure was also applied at OHP with the star HD 160952 (G8III). Note that the use of a cold giant is a valuable criterion for a cross-correlation procedure since the profile of strong lines such as K, H, G, Hβ, or MgIb is not affected by gravity and/or metal abundance; it remains narrow, with a Doppler core and Stark-broadened wings (Praderie 1967); galaxies templates with good measured radial velocities given by Lauberts & Valentijn (1989) were also observed in the same conditions, in order to use real galaxies as templates in the cross-correlation procedure.

The data reduction was carried out using the IRAF package; Wavelength calibration was performed using the He-Ar (ESO) and He-Ne (OHP) lamp references. The spectra were rebinned with a scale of 1 Å/bin equally spaced in log wavelength and the velocity was derived from the cross-correlation procedure with stellar and galaxy template spectra of known radial velocity obtained the same night, according to Tonry & Davis (1979). We used the RVSAO package developped at Harvard (Kurtz et al. 1991; Mink et al. 1995). Table 1 lists positions and heliocentric velocities for 65 individual galaxies in the four clusters:

1. Dressler (1980) number
2. alternative name IC or MCG
3. right ascension (hour, min, s)
4. declination (degree, minute, second)
5. morphological type from Dressler's (1980) catalogue
6. estimated total apparent visual magnitude (Dressler 1980)
7. heliocentric radial velocity with its error in $\mathrm{km\,s^{-1}}$
8. instrumentation and notes, **e**: 1.50 m ESO telescope, **o**: 1.93 m OHP telescope + CARELEC spectrograph, **s**: 1.93 m telescope + SILFID spectrograph.

In order to test the external accuracy of our velocities, we compared our redshift determinations with data available in the literature for the same set of galaxies.

Comparisons
were made separately for each galaxy cluster. We obtain respectively $< V_o - V_{ref} >= -13.0\ \mathrm{km\,s^{-1}}$, the standard deviation in the difference being $59\ \mathrm{km\,s^{-1}}$ for A 957 (data from Beers et al. 1991), $< V_o - V_{ref} >= -34.1\ \mathrm{km\,s^{-1}}$, with $\sigma = 65\ \mathrm{km\,s^{-1}}$ for A 2040 (data from Zabludoff et al. 1993), and $< V_o - V_{ref} >= 14.4\ \mathrm{km\,s^{-1}}$, with $\sigma = 59\ \mathrm{km\,s^{-1}}$ for A 2063 (data from Beers et al. 1991). All these results are consistent with the errors of Table 1. The velocities in the present study agree with those previously published within the 2 σ level.

Table 2 lists the positions and heliocentric velocities for 15 individual galaxies observed separately through the galactic plane in July 1991.

3. Discussion

3.1. *Velocity analysis*

Including previous measurements in the same clusters (Proust et al. 1987; Capelato et al. 1991; Beers et al. 1991; Zabludoff et al. 1993, and few other data from literature, there is for A 957, A 979, A 2040 and A 2063 a total of 128 velocities. The new measurements presented here together with those collected in the literature allow the constitution of samples whose completeness up to the limiting magnitude of Dressler's (1980) catalogue ($m_v = 16$) ranges about 67 to 88% in their central core regions. They are all cD or D-galaxy dominated clusters. For these clusters we present below a dynamical analysis based on these samples.

3.2. *A 957*

A total of 40 redshifts have been measured for this cluster (Proust et al. 1987; Capelato et al. 1991; Beers et al. 1991, this paper). The projected distribution of galaxies is displayed with different symbols in Fig. 1. The sample of measured radial velocities is 89% complete within a circular region of 16.0 arcmin radius ($0.64 h_{100}^{-1}$ Mpc) centered on the D galaxy, the brightest member of the cluster. This sample contains 32 galaxies and covers the elongated central condensation of A 957. Its mean velocity is $\overline{V} = 13305 \pm 160\ \mathrm{km\,s^{-1}}$ with a velocity dispersion $\sigma = 846^{+135}_{-92}\ \mathrm{km\,s^{-1}}$. If we consider the morphological types, the mean velocities and the velocity dispersions are: $\overline{V} = 13286\ \mathrm{km\,s^{-1}}$ $\sigma = 719\ \mathrm{km\,s^{-1}}$ for E + S0 galaxies (24 objects) and $\overline{V} = 13517\ \mathrm{km\,s^{-1}}$ $\sigma = 1476\ \mathrm{km\,s^{-1}}$ for S + I galaxies (8 objects). Note that although the mean velocities of early and late-type galaxies are similar, the latter have a velocity dispersion much larger than the former. This may result from the 3 galaxies with velocities greater than $14000\ \mathrm{km\,s^{-1}}$. If not due to interlopers, this result may be interpreted as an evidence that late-type galaxies are still in the process of infalling towards a virialized core (Sodré et al. 1989). Figure 2 shows the histograms for the measured velocities between 11000 and $16000\ \mathrm{km\,s^{-1}}$ for S + I (up), and E + S0 (down) galaxies and Fig. 3 shows the wedge velocity diagram of the cluster in right ascension (up) and declination (down). Note that the velocity distribution obtained with a larger set of velocities does not confirm the relative depletion of galaxies with $v \simeq 13000\ \mathrm{km\,s^{-1}}$ proposed by Capelato et al. (1991).

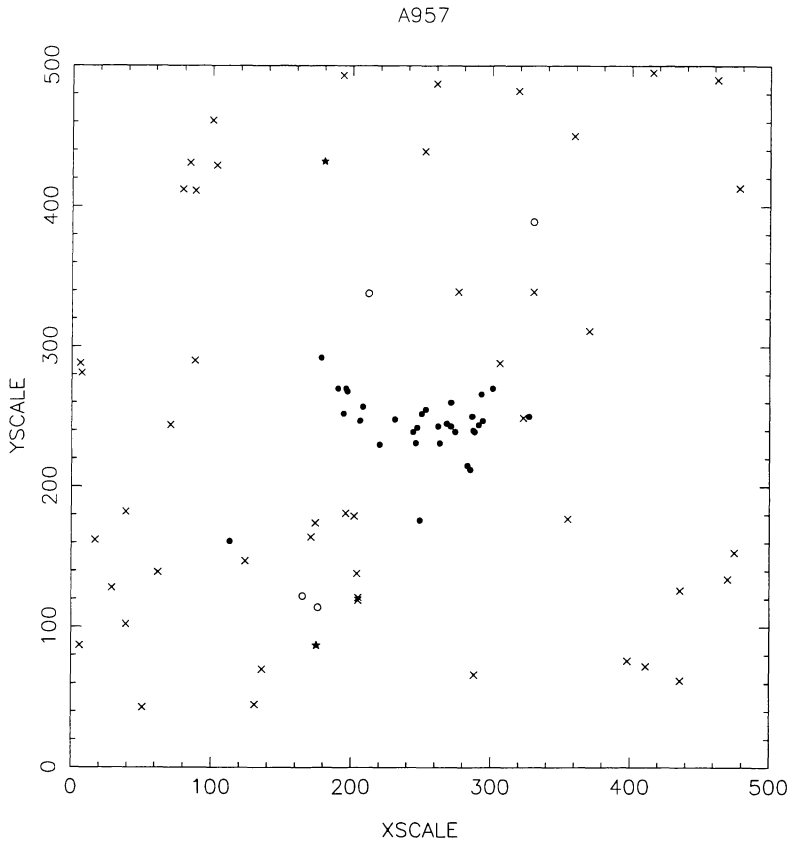

Fig. 1. Galaxy positions of the A 957 cluster symbolized by a circle for objects with $V_r > 16000$ km s^{-1}, filled dot with $11500 \leq V_r < 16000$ km s^{-1}, and filled star with $V_r < 11500$ km s^{-1}; non measured objects are represented by a cross

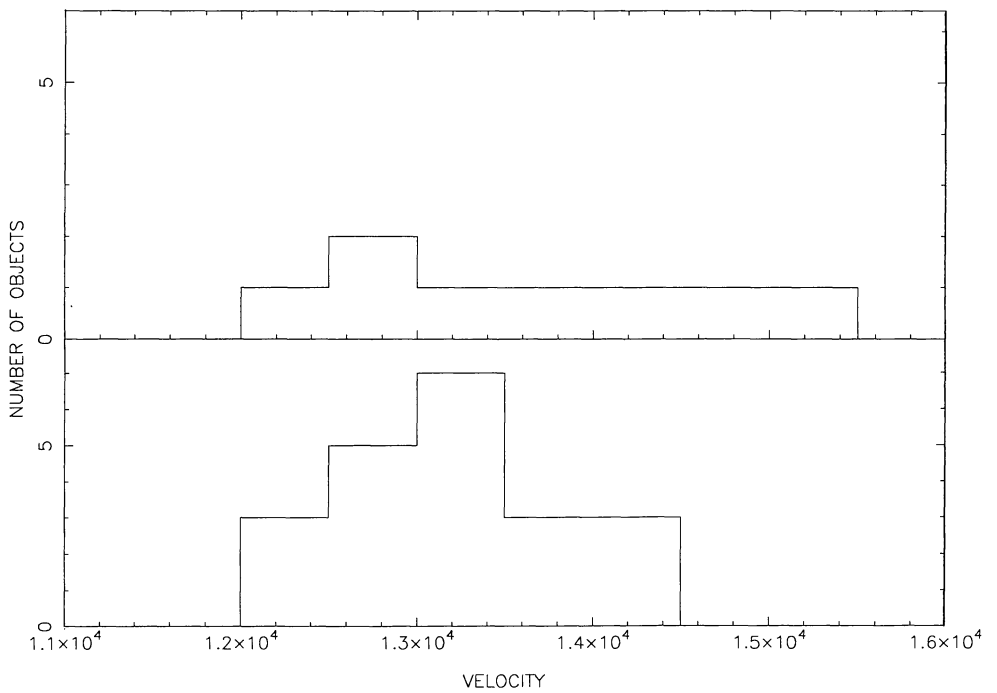

Fig. 2. Velocity histograms for the measured velocities between 11000 and 16000 km s^{-1} for S + I (up), and E + S0 (down) galaxies in the central part of A 957

Table 1. Heliocentric redshifts for galaxies

GALAXY	NAME	R.A. (1950)	DEC. (1950)	TYPE	MAG.	HEL. VEL. $V\pm\Delta V$	N
A 957							
31		10 10 58.5	-00 45 00	E	15.0	12333 63	s
33		10 11 44.2	-00 42 13	S0	16.0	13812 63	s
36		10 11 13.5	-00 39 53	Sc	14.0	12862 56	s
37		10 11 13.0	-00 42 07	S0	15.0	12812 49	s
38		10 11 06.7	-00 39 57	E	16.0	12876 61	s
39	MCG-0-26-30	10 11 04.9	-00 40 34	D	13.0	13277 59	s
40		10 10 55.4	-00 40 26	E	16.0	12836 78	s
41		10 10 54.7	-00 40 41	S	16.0	11656 89	s
42		10 10 52.3	-00 39 41	S0	15.0	12588 54	s
43		10 11 52.3	-00 37 20	S0	15.0	14465 52	s
48		10 11 20.1	-00 37 40	E/S0	16.0	13978 102	s
49		10 11 08.7	-00 39 28	S0	16.0	13232 88	s
50		10 11 06.8	-00 36 53	S0	16.0	13515 69	s
51		10 10 55.4	-00 38 36	S0	16.0	12471 59	s
58		10 12 00.8	-00 35 12	S0	16.0	13334 67	s
59		10 10 50.9	-00 35 40	SB0	16.0	12768 77	s
A 979							
01		10 20 25.5	-08 20 37	Sa	16.0	16088 44	e1
04		10 18 05.0	-08 20 27	E/S0	15.0	16471 24	e
07		10 17 36.8	-08 21 02	Sa	15.0	16355 27	e
20		10 18 40.1	-07 54 59	Sab	15.0	10282 89	e
21		10 17 26.7	-07 53 05	Sbc	15.0	15736 61	o
26		10 17 51.6	-07 48 12	E	15.0	16296 41	o
36		10 18 56.7	-07 40 10	Sab	15.0	11360 78	e
39	MCG-1-27-01	10 17 49.9	-07 38 30	D	14.0	16526 37	e
42		10 18 19.8	-07 36 39	SBb	15.0	9392 59	e2
44		10 17 45.2	-07 38 06	SBa/0	15.0	15010 54	e
45		10 17 41.5	-07 35 47	E	15.0	16158 17	o
46		10 17 21.7	-07 35 35	E	16.0	15986 43	e
48		10 19 41.2	-07 33 13	I	16.0	16356 41	e
49		10 18 34.3	-07 31 38	E	15.0	15473 53	e
51		10 17 48.7	-07 32 38	S	16.0	15631 78	e
52		10 17 38.4	-07 31 44	Sa	15.0	15413 57	e
53		10 17 34.9	-07 33 47	S/I	16.0	18657 26	o3
55		10 17 03.1	-07 31 34	E	16.0	23147 34	e
57		10 18 52.0	-07 29 34	Sa/0	15.0	16477 58	e
59		10 18 06.3	-07 29 30	E/S0	15.0	16242 39	e
61		10 19 11.3	-07 25 33	S0/a	15.0	10948 49	e
72		10 18 28.9	-07 13 41	Sa	14.0	11807 76	e4

Estimates for dynamical mass of A 957 using the mass estimators for self-gravitating systems of equal-mass galaxies with velocities $11000 \leq V < 16000$ km s^{-1}, as derived from Heisler et al. (1985) are listed in Table 3.

3.3. *A 979*

A total of 22 redshifts have been obtained for A 979. Figure 4 shows with different symbols the relative positions of galaxies with and without measured radial velocities (here as in the following the x-y positions of galaxies have been taken from Dressler's catalogue (1980) and Fig. 5 shows the wedge velocity diagram of the cluster in right ascension (up) and declination (down). The cluster is probably part of a large structure since the available velocities indicate the presence of foreground ($V_r < 15000$ km s^{-1}) and background ($V_r > 18000$ km s^{-1}) galaxies. The 5 foreground galaxies with $\overline{V} = 10758$ km s^{-1} form a substructure, as suggested by West & Bothun (1990). Considering the 15 galaxies with radial velocities between 15000 and 18000 km s^{-1}, the cluster mean velocity is $\overline{V} = 16015 \pm 119$ km s^{-1} with a corrected velocity

Table 1. continued

GALAXY	NAME	R.A. (1950)	DEC. (1950)	TYPE	MAG.	HEL. VEL. $V\pm\Delta V$	N
A 2040							
48		15 10 42.8	+07 37 28	S0	15.0	14102 67	s
49		15 10 23.8	+07 36 42	S0/E	15.0	13668 36	o
50		15 10 20.1	+07 36 47	S0	16.0	13752 64	s
51		15 10 20.5	+07 37 16	D	14.0	13683 15	o
51						13721 69	s
52		15 10 20.1	+07 38 25	S0	16.0	12854 74	o
53		15 10 16.3	+07 38 04	S0/E	16.0	13098 78	o
54		15 10 10.5	+07 38 20	S0	16.0	31958 59	o
55		15 10 07.4	+07 37 08	Ep	15.0	12794 79	s
57		15 13 05.2	+07 39 37	Sa/0	15.0	13723 67	s
A 2063							
24		15 22 03.6	+08 32 59	SBb	14.0	10987 62	s
36	IC1116	15 19 29.1	+08 36 08	E/S0	13.0	11698 59	s
37		15 19 14.2	+08 35 39	SBc	14.0	11588 61	s
38		15 18 27.0	+08 34 35	Sa	14.0	9355 53	s
43		15 20 34.2	+08 38 35	SBb	16.0	9122 91	s
45		15 20 06.0	+08 40 27	S0	16.0	11675 89	s
46		15 20 44.6	+08 40 59	S0	15.0	10721 67	s
49		15 20 46.6	+08 43 41	Sb	15.0	10895 89	s
50	MCG+2-39-21	15 20 41.0	+08 42 23	S0	15.0	9851 65	s
52		15 20 29.9	+08 41 57	Sb	15.0	11532 83	s
58	MCG+2-39-25	15 20 54.5	+08 47 46	S0/a	15.0	10773 54	s
59	MCG+2-39-22	15 20 49.1	+08 45 03	S0	15.0	10413 78	s
60	MCG+2-39-20	15 20 39.5	+08 47 14	D	13.0	10593 62	s
61		15 20 38.9	+08 47 24	S0	16.0	10389 88	s
62		15 20 36.8	+08 46 52	E	16.0	10799 89	s
65		15 19 52.4	+08 45 30	S0	16.0	10956 79	s
72		15 20 48.2	+08 49 22	E	15.0	10530 61	s

emission lines. **1**: H_β = 16106 km s^{-1}, H_α = 16046 km s^{-1}; **2**: H_α = 9355 km s^{-1}; **3**: OII= 18710 km s^{-1}; **4**: H_β = 11919 km s^{-1}, H_α = 11939 km s^{-1}.

Table 2. Galaxies observed through the galactic plane at OHP

GALAXY	NAME	R.A. (1950)	DEC. (1950)	TYPE	MAG.	DIAM. $V\pm\Delta V$	HEL. VEL.	N
ZW255-25	MCG 8-34-33	19 02 01.0	45 32 17		15.	0.4x0.7	5372 51	
ZW229-15		19 03 50.8	42 23 01	Seyfert1	15.4		8358 22	1
ZW256-05		19 05 36.0	46 05 54		15.3		6375 71	
ZW229-18		19 05 42.4	39 51 04		15.5		8463 39	
ZW229-21	MCG 7-39-13	19 06 45.0	42 59 17	Sc	14.7	1.1x2.0	4563 37	
ZW229-23		19 07 07.3	43 15 42		15.2		16084 73	
ZW229-25	MCG 7-39-15	19 07 47.0	42 58 56		14.8		4618 30	
ZW230-20		19 29 08.1	41 11 53		14.6		4914 61	
ZW230-22	MCG 7-40-10	19 30 46.4	41 47 45		14.8	1.0x1.0	9037 48	
ZW256-20		19 32 45.7	49 09 34		15.4		7869 57	
UGC11460	MCG 7-40-12	19 36 11.1	40 53 40	E/S0	14.0	0.8x1.2	4607 39	
ZW257-17		19 49 26.1	47 55 51		14.9		7781 50	
ZW257-18		19 50 34.4	47 59 49		15.0		7915 61	
IRAS 203525		20 35 09.5	25 21 11				10268 54	
ZW448-06		20 45 24.0	20 36 00		15.3		10506 67	

(1): emission lines: Hγ, Hβ, 2*OIII.

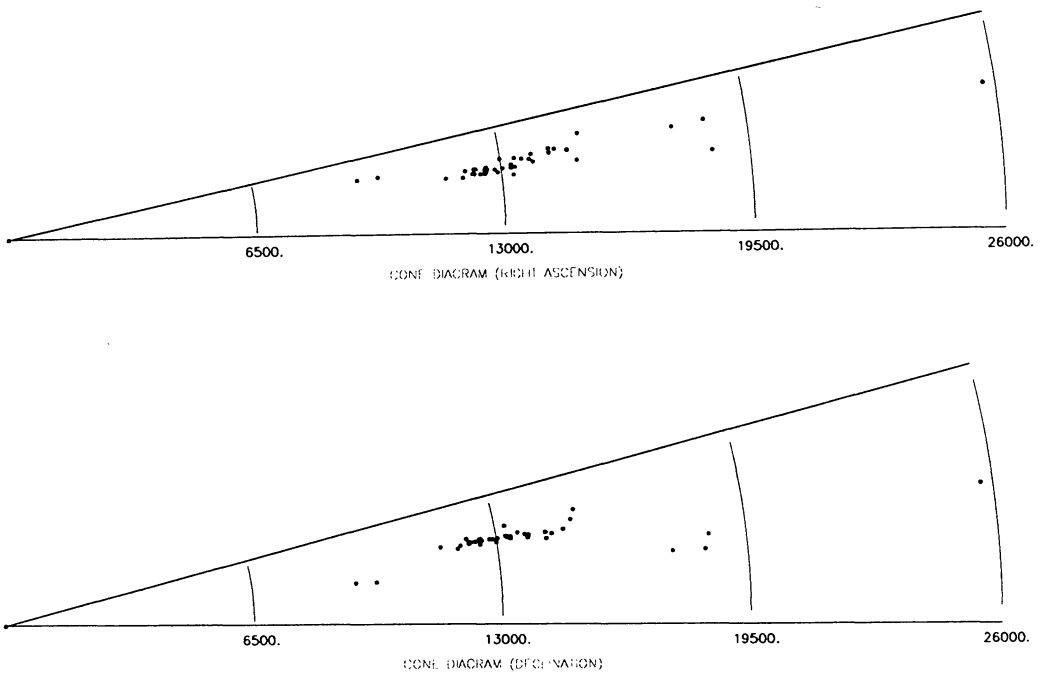

Fig. 3. Wedge velocity diagram in right ascension (up), and declination (down) for the measured galaxies in A 957

Table 3. Dynamical mass estimations of A 957 in ($10^{14} M_{\odot}$)

	mass	error
VIRIAL MASS	3.42	
PROJECTED MASS	7.70	0.89
AVERAGE MASS	5.66	0.40
MEDIAN MASS	2.69	0.21

Table 4. Dynamical mass estimations of A 979 in ($10^{14} M_{\odot}$)

	mass	error
VIRIAL MASS	2.53	
PROJECTED MASS	3.40	0.87
AVERAGE MASS	2.77	0.46
MEDIAN MASS	2.20	0.39

dispersion $\sigma = 426^{+113}_{-67}$ km s^{-1} (confidence level= 68%). The uncertainties were calculated following Danese et al. (1980), assuming a mean observational error on individual radial velocities of 100 km s^{-1}. If we consider the morphological types, the mean velocities and velocity dispersions are: $\overline{V} = 16217$ km s^{-1} $\sigma = 352$ km s^{-1} for E + S0 galaxies (7 objects) and $\overline{V} = 15837$ km s^{-1} $\sigma = 490$ km s^{-1} for S + I galaxies (8 objects).The most interesting result about this cluster is that the D galaxy has a large peculiar velocity compared with the cluster mean: $\frac{V_D - \overline{V}}{\sigma} = 1.2$. We obtain a mean cluster distance of 156 Mpc assuming $H_0 = 100$ km s^{-1} Mpc^{-1} and $q_0 = 0.1$. The Abell radius of 35 arcmin corresponds to 1.51 Mpc. Estimates of the dynamical mass of A 979 are listed in Table 4.

3.4. *A 2040*

A total of 34 redshifts have been measured for this cluster (Capelato et al. 1991; Zabludoff et al. 1993, this paper). The projected distribution of galaxies is displayed with different symbols in Fig. 6. Note that there is a group along the line of sight with velocities around 10000 km s^{-1}. The main cluster contains 25 measured galaxies with $\overline{V} = 13510 \pm 78$ km s^{-1} with a dispersion velocity $\sigma = 361^{+68}_{-47}$ km s^{-1}. From the morphological types, the mean velocities and velocity dispersions are: $\overline{V} = 13487$ km s^{-1} $\sigma = 373$ km s^{-1} for E + S0 galaxies (16 objects) and $\overline{V} = 13552$ km s^{-1} $\sigma = 439$ km s^{-1} for S + I galaxies (9 objects). Figure 7 shows the wedge velocity diagram of the cluster in right ascension (up) and declination (down). Estimates of the dynamical mass of A 2040 are listed in Table 5.

3.5. *A 2063*

Including data from literature (Beers et al. 1991; Capelato et al. 1991; Zabludoff et al. 1993), there are a total of 44 known redshifts for A 2063. Figure 8 shows with different symbols the relative positions of galaxies with and without measured radial velocities and Fig. 9 shows the

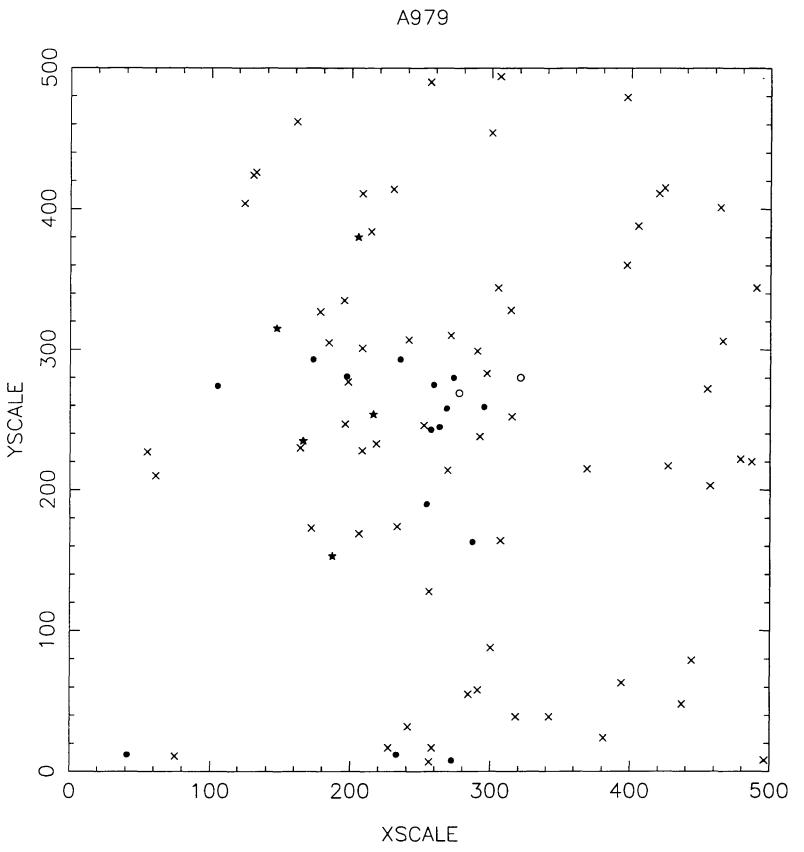

Fig. 4. Galaxy positions of the A 979 cluster symbolized by a circle for objects with $V_r > 18000$ km s^{-1}, filled dot with $15000 \leq V_r < 18000$ km s^{-1}, and filled star with $9000 \leq V_r < 15000$ km s^{-1}; non measured objects are represented by a cross

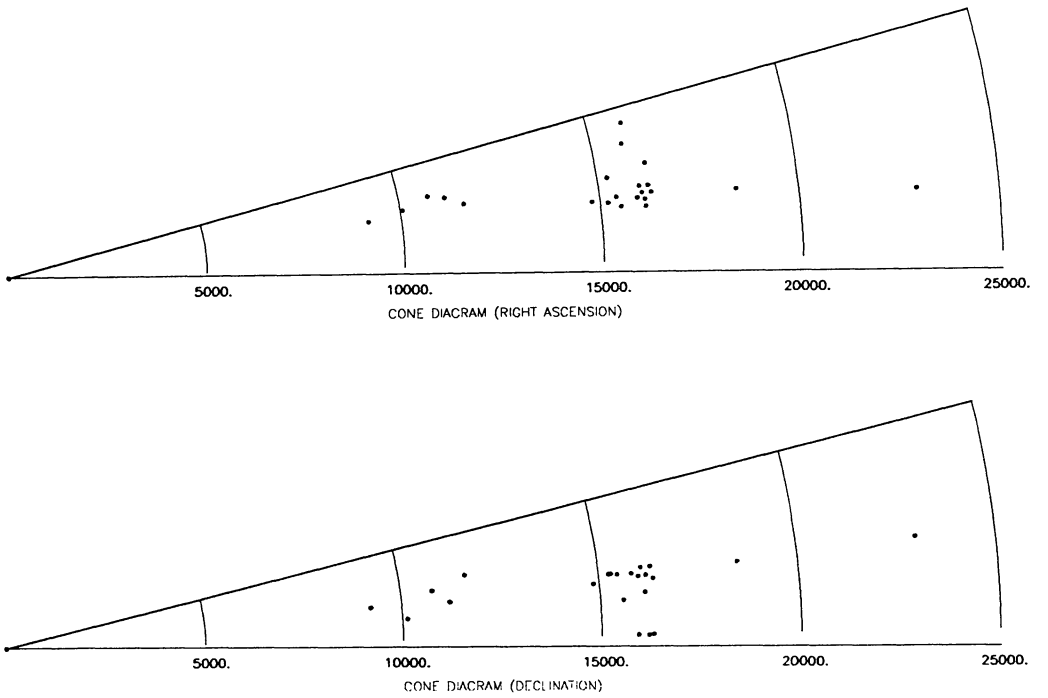

Fig. 5. Wedge velocity diagram in right ascension (up), and declination (down) for the measured galaxies in A 979

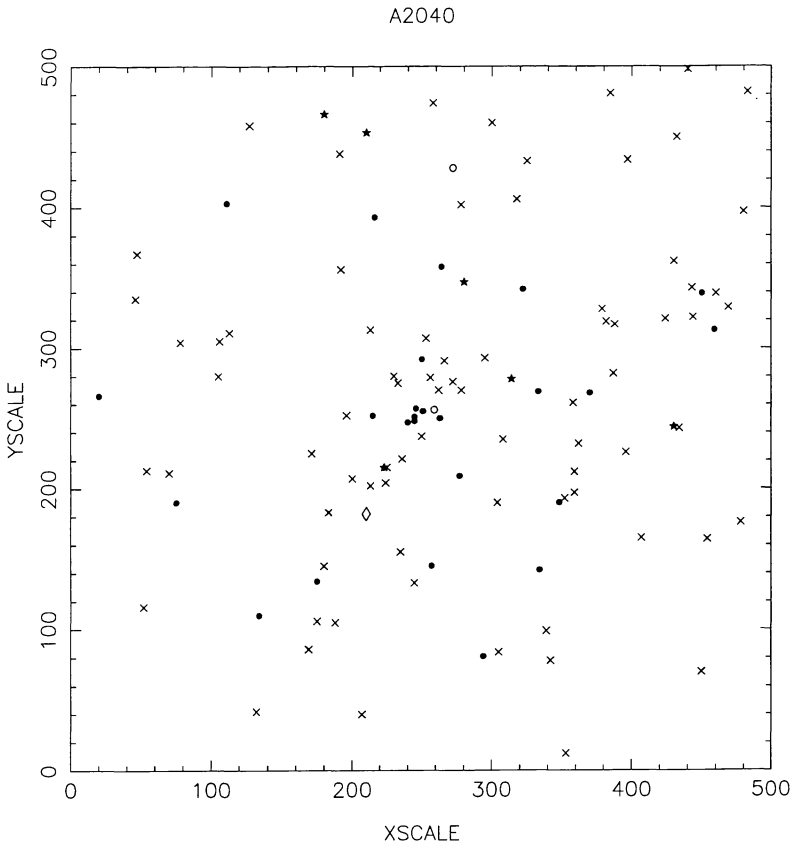

Fig. 6. Galaxy positions of the A 2040 cluster symbolized by a circle for objects with $V_r > 15000$ km s^{-1}, filled dot with $12000 \leq V_r < 15000$ km s^{-1}, and filled star with $9000 \leq V_r < 12000$ km s^{-1}; non measured objects are represented by a cross. The foreground galaxy 22 is symbolized by a diamond

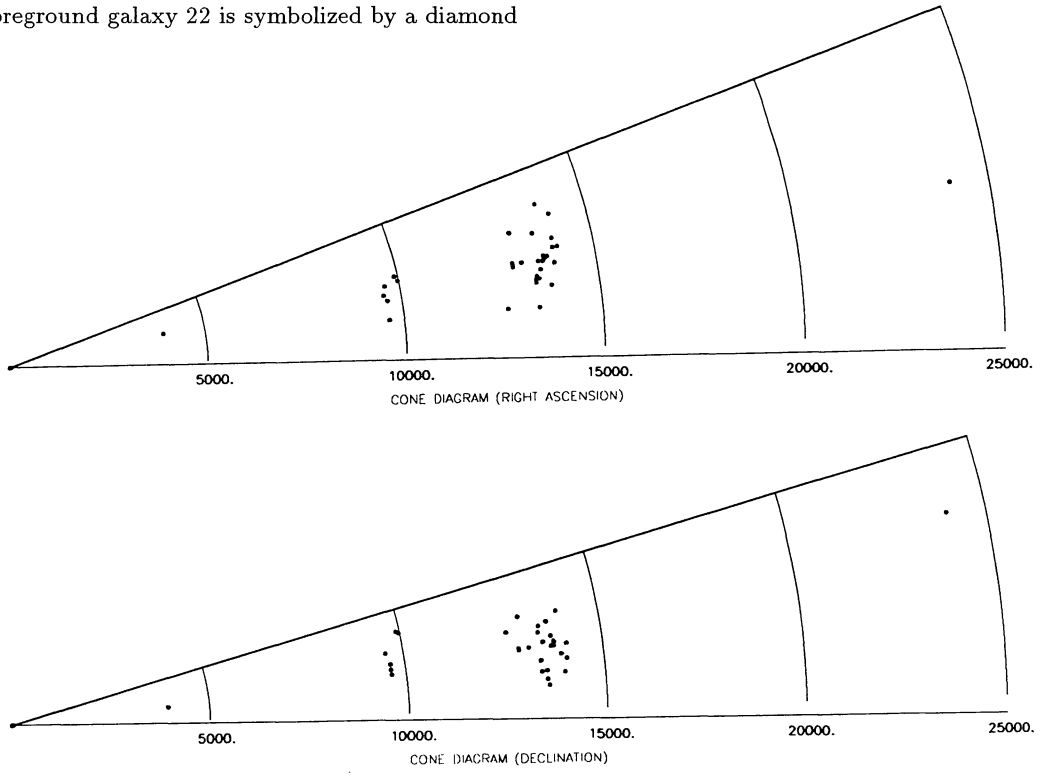

Fig. 7. Wedge velocity diagram in right ascension (up), and declination (down) for the measured galaxies in A 2040

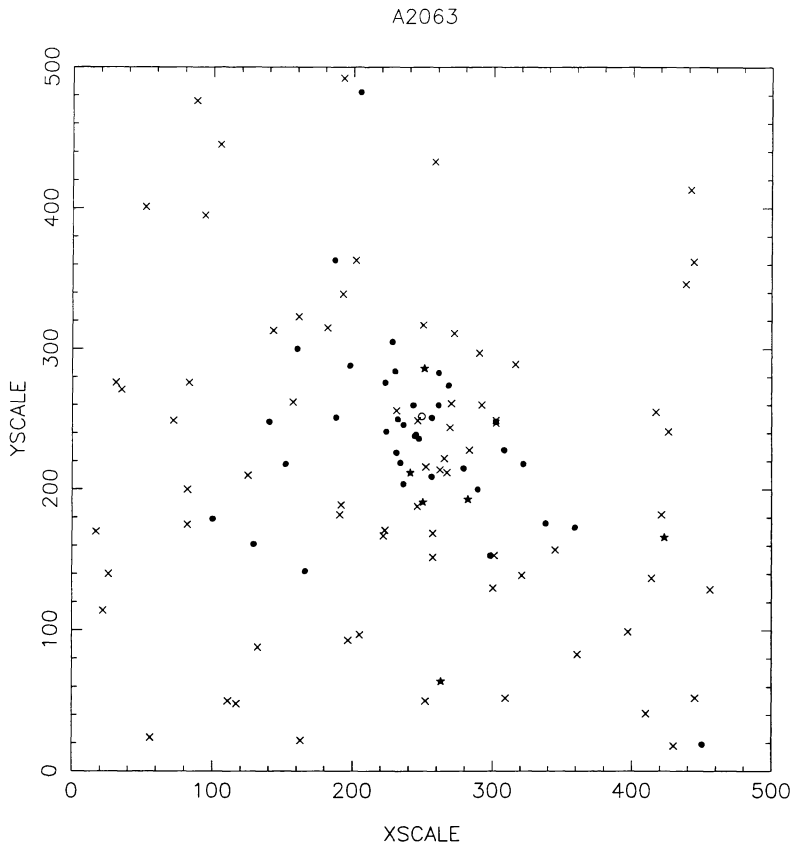

Fig. 8. Galaxy positions of the A 2063 cluster symbolized by a circle for objects with $V_r > 15000$ km s^{-1}, filled dot with $10000 \leq V_r < 13500$ km s^{-1}, and filled star with $9000 \leq V_r < 10000$ km s^{-1}; non measured objects are represented by a cross

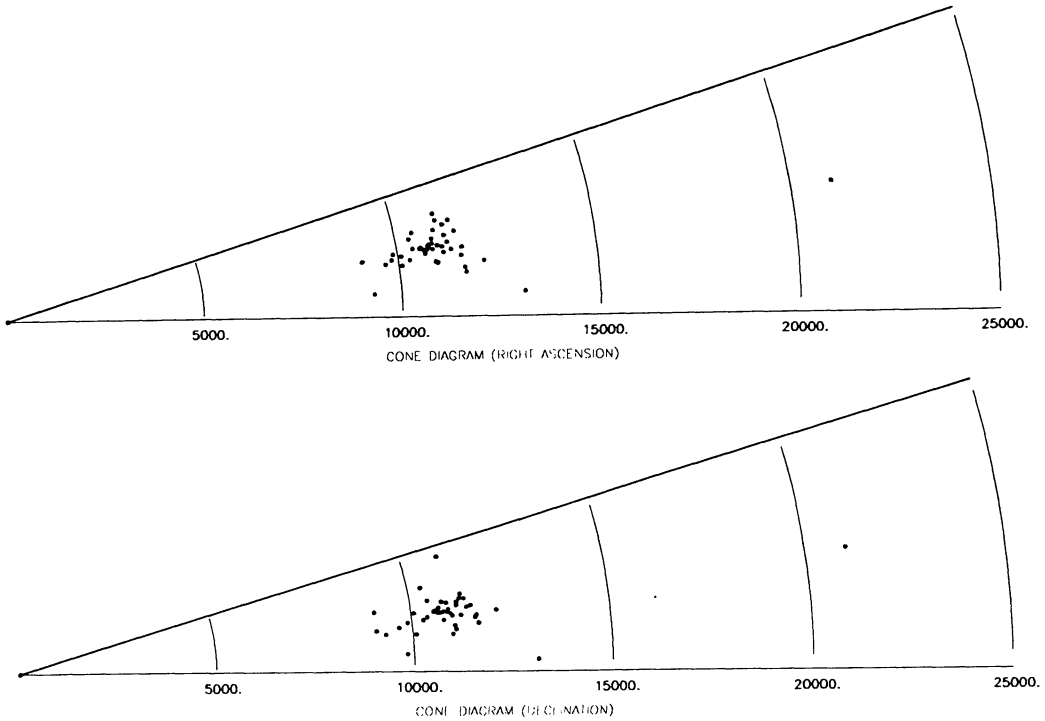

Fig. 9. Wedge velocity diagram in right ascension (up), and declination (down) for the measured galaxies in A 2063

Table 5. Dynamical mass estimations of A 2040 in ($10^{14} M_{\odot}$)

	mass	error
VIRIAL MASS	1.61	
PROJECTED MASS	2.80	0.50
AVERAGE MASS	2.32	0.19
MEDIAN MASS	1.53	0.12

wedge velocity diagram of the cluster in right ascension (up) and declination (down). Note that the presence of a clump of foreground galaxies with $V < 10000$ km s^{-1} is questionable. The main cluster contains 34 measured galaxies with $\overline{V} = 10767 \pm 118$ km s^{-1} with a velocity dispersion $\sigma = 741^{+97}_{-71}$ km s^{-1}. From the morphological types, the mean velocities and velocity dispersions are: $\overline{V} = 10746$ km s^{-1} $\sigma = 558$ km s^{-1} for E + S0 galaxies (28 objects) and $\overline{V} = 10805$ km s^{-1} $\sigma = 1093$ km s^{-1} for S + I galaxies (15 objects). Estimates of the dynamical mass of A 2063 are listed in Table 5.

Table 6. Dynamical mass estimations of A 2063 in ($10^{14} M_{\odot}$)

	mass	error
VIRIAL MASS	3.95	
PROJECTED MASS	9.02	1.21
AVERAGE MASS	6.15	0.52
MEDIAN MASS	2.75	0.18

4. Conclusion

In this paper, we have reported new measurements on the A 957, A 979, A 2040 and A 2063 clusters of galaxies. This allowed us to define almost complete samples of galaxies in the central part of the four cD clusters, and to discuss the nature of these clusters. However the very precise determinations on the shape of the velocity-dispersion profile can only be obtained by removing the effects of contamination and subclustering. Our dynamical analyses suggest that the four clusters have similar masses, a few times ($10^{14} M_{\odot}$). It is also of interest to point out the large peculiar velocity of the D galaxy in A 979, which is not easily explained by the usual models of formation of this type of galaxy (Merritt 1984). Finally we note that for A 957 and A 2063, the velocity dispersion of late-type galaxies seems larger than that of the early-type ones. If not due to interlopers, this result is in agreement with the idea that spirals are infalling onto a virialized core composed of elliptical and lenticular galaxies (Sodré et al. 1989).

Acknowledgements. We thank the OHP and ESO staff, and especially Hugo Schwartz, Patrice Bouchet and Daniel Hofstadt. LSJ thanks the financial support provided by FAPESP and CNPq.

References

Beers T.C., Forman W., Huchra J.P., Jones C., Gebhardt K., 1991, AJ 102, 1581
Capelato H.V, Mazure A., Proust D., et al., 1991, A&AS 90, 355
Danese L., De Zotti G., di Tullio G., 1980, A&A 82, 322
Dressler A., 1980, ApJS 42, 565
Heisler J., Tremaine S., Bahcall J.N., 1985, ApJ 298, 8
Kraan-Korteweg R.C, Cayatte V., Balkowski C., Fairall A.P., Henning P.A., 1994, ASP Conf. Ser. 67, 99
Kurtz M.J., Mink D.J., Wyatt W.F., Fabricant D.G., Torres G., Kriss G.A., Tonry J.L., 1991, ASP Conf. Ser. 25, 432
Lauberts A., Valentijn E.A., 1989, The Surface Photometry Catalogue of the ESO-Uppsala Galaxies, ESO
Maurice E., Mayor M., Andersen J., et al., 1984, A&AS 57, 275
Merritt D., 1984, ApJ 276, 26
Mink D.J., Wyatt W.F., 1995, ASP Conf. Ser. 77, 496
Praderie F., 1967, Ann. Astrophys. 29, 601
Proust D., Talavera A., Salvador-Solé E., Mazure A., Capelato H.V., 1987, A&AS 67, 57
Proust D., Mazure A., Sodré L., Capelato H., Lund G., 1988, A&AS 72, 415
Proust D., Quintana H., Mazure A., et al., 1992, A&A 258, 243
Sodré L., Capelato H.V., Steiner J.E., Mazure A., 1989, AJ 97, 1279
Tonry J., Davis M., 1979, AJ 84, 1511
Vanderriest C., Lemonnier J.P., 1988, in Instrumentation for ground-based Optical Astronomy, proc. IXth Santa Cruz workshop, p. 304
West M.J., Bothun G.D., 1990, ApJ 350, 36
Zabludoff A.I., Geller M.J., Huchra J.P., Vogeley M.S., 1993, AJ 106, 1273